which are known to control aspects of plant development. The *AG* MADS-box gene has a critical function in plant sexual reproduction, because *ag* mutants completely lack reproductive organs. However, because *AG* is only one of four members of a monophyletic clade, it has been necessary to characterize all possible combinations of single, double, triple and quadruple mutants. Now that the individual and redundant roles of the *AG* clade of MADS-box genes are known, we can begin to explore their roles in setting up the patterns of downstream gene expression required for carpel and ovule development. □

Methods

Reporter construct and histology

The STK::*GUS* reporter construct is a translational fusion of sequence 2 kilobases (kb) upstream of the *STK* translation start codon with the GUS (uidA) gene in pDW137 (ref. 17). The sequence was amplified by primer P1 (5′-CCTGCAGCCGTGATTGCAATT GCAAAATTTGAG-3′) and P5 (5′-CTCTAGACCCATCCTTCATTTTAAACA-3′) then cloned into pCRII vector, yielding pPOP163. This 2-kb sequence contains 1.3 kb of the first intron and 0.7 kb of the promoter region. The sequence was then cloned into the *Pst*I and *Xba*I sites of pDW137, resulting in pPOP166. GUS staining was performed as described previously[18] except that the concentrations of potassium ferrocyanide and potassium ferricyanide were 5 mM.

Plant materials

The *stk-1* allele was identified by screening for an *En-1* insertion among a collection of plants carrying about 50,000 independent insertions by using the *STK*-specific primer 11-X5 (5′-CCACTAACCATTTGATGATGGTGTTGT-3′) and the *En-1*-specific primer En8130 (5′-GAGCGTCGGTCCCCACACTTCTATAC-3′)[19]. *En-1* is inserted near the 3′ end of exon 3 (2 base pairs (bp) from the splice site). The *stk-2* and *stk-3* stable alleles were obtained by screening for germinal excision of the *stk-1* allele. The s*tk-2* allele contains a 74-bp insertion near the splice site of third intron. The *stk-3* allele has a 47-bp deletion that removes the splice site. Analysis by polymerase chain reaction (PCR) with reverse transcription showed that mutations in both alleles affected RNA splicing (data not shown). Two additional mutant alleles, *stk-4* and *stk-5*, were obtained from the Madison Alpha collection by using the gene-specific primers 11-X15 (5′-TTCTTGCAGTCTGCC ACTAGTTTGTGTGT-3′) and 11-X18 (5′-AACTGCTTCGTTACGCACCGAACTCA ACA-3′), respectively, together with the T-DNA-specific primer JL202 (5′-CATTTTATA ATAACGCTGCGGACATCTAC-3′). The *stk shp1 shp2* triple mutants were generated by crossing *shp1-1 shp2-1* double-mutant plants with plants carrying either the *stk-2* or the *stk-3* allele. The *shp* alleles[10,20] *ap2-6* (ref. 21) and *ag-2* (ref. 22) used for generating the mutants were described previously. The 35S:*SHP1/2* transgenic plants were described previously[10]. The 35S:*SHP2* transgene was introduced into *ag-1* mutants.

Mutant genotyping

The *stk-2* and *stk-3* alleles were genotyped by PCR with the primers 11-x4 (5′-GCTTGTTCTGATAGCACCAACACTAGCA-3′) and 11-x5 (5′-CCACTAACCATTTGAT GATGGTGTTGT-3′). The *stk shp1 shp2* triple mutants were identified by screening for mutant phenotypes and later confirmed by PCR genotyping all three genes. Genotyping of *shp1-1* and *shp2-1* allele was as described previously[10]. The *ap2-6* allele was genotyped by PCR amplification with the primers G1021 (5′-GCAGCAGCTCGGTATTTTTC-3′) and G1022 (5′-ATCAAACCGGTGGTTCTCAG-3′) followed by digestion with *Hin*dIII. The *Hin*dIII site is present only in the *ap2-6* allele.

Scanning electron microscopy

Flowers and fruits were fixed overnight in 1.6% osmium tetroxide in 50 mM sodium cacodylate buffer at 4 °C. Tissues were washed twice in the same buffer and dehydrated in an acetone series. After critical-point drying, pistils and fruits were dissected to expose ovules or seeds inside. Tissues were coated with gold/palladium. Samples were examined in either a Cambridge S360 scanning electron microscope or a Quanta 600 microscope using an acceleration voltage of 5–20 kV.

Received 26 February; accepted 1 May 2003; doi:10.1038/nature01741.

1. Bowman, J. L., Smyth, D. R. & Meyerowitz, E. M. Genes directing flower development in *Arabidopsis*. *Plant Cell* **1,** 37–52 (1989).
2. Bowman, J. L., Smyth, D. R. & Meyerowitz, E. M. Genetic interactions among floral homeotic genes of *Arabidopsis*. *Development* **112,** 1–20 (1991).
3. Theissen, G. *et al.* A short history of MADS-box genes in plants. *Plant Mol. Biol.* **42,** 115–149 (2000).
4. Stewart, W. N. & Rothwell, G. W. *Paleobotany and the evolution of plants* (Cambridge Univ. Press, 1993).
5. Drews, G. N., Bowman, J. L. & Meyerowitz, E. M. Negative regulation of the *Arabidopsis* homeotic gene *AGAMOUS* by the *APETALA2* product. *Cell* **65,** 991–1002 (1991).
6. Alvarez, J. & Smyth, D. R. *CRABS CLAW* and *SPATULA*, two *Arabidopsis* genes that control carpel development in parallel with *AGAMOUS*. *Development* **126,** 2377–2386 (1999).
7. Savidge, B., Rounsley, S. D. & Yanofsky, M. F. Temporal relationship between the transcription of two *Arabidopsis* MADS box genes and the floral organ identity genes. *Plant Cell* **7,** 721–733 (1995).
8. Flanagan, C. A., Hu, Y. & Ma, H. Specific expression of the *AGL1* MADS-box gene suggests regulatory functions in *Arabidopsis* gynoecium and ovule development. *Plant J.* **10,** 343–353 (1996).
9. Heisler, M. G. B., Atkinson, A., Bylstra, Y. H., Walsh, R. & Smyth, D. R. *SPATULA*, a gene that controls development of carpel margin tissues in *Arabidopsis*, encodes a bHLH protein. *Development* **128,** 1089–1098 (2001).
10. Liljegren, S. J. *et al. SHATTERPROOF* MADS-box genes control seed dispersal in *Arabidopsis*. *Nature* **404,** 766–770 (2000).
11. Mizukami, Y. & Ma, H. Ectopic expression of the floral homeotic gene *AGAMOUS* in transgenic *Arabidopsis* plants alters floral organ identity. *Cell* **71,** 119–131 (1992).
12. Rounsley, S. D., Ditta, G. S. & Yanofsky, M. F. Diverse roles for MADS box genes in *Arabidopsis* development. *Plant Cell* **7,** 1259–1269 (1995).
13. Ma, H., Yanofsky, M. F. & Meyerowitz, E. M. *AGL1-AGL6*, an *Arabidopsis* gene family with similarity to floral homeotic and transcription factor genes. *Genes Dev.* **5,** 484–495 (1991).
14. Angenent, G. C. *et al.* A novel class of MADS box genes is involved in ovule development in *Petunia*. *Plant Cell* **7,** 1569–1582 (1995).
15. Colombo, L. *et al.* The *Petunia* MADS box gene *FBP11* determines ovule identity. *Plant Cell* **7,** 1859–1868 (1995).
16. Western, T. L. & Haughn, G. W. *BELL1* and *AGAMOUS* genes promote ovule identity in *Arabidopsis thaliana*. *Plant J.* **18,** 329–336 (1999).
17. Blazquez, M. A., Soowal, L. N., Lee, I. & Weigel, D. *LEAFY* expression and flower initiation in *Arabidopsis*. *Development* **124,** 3835–3844 (1997).
18. Sessions, A., Weigel, D. & Yanofsky, M. F. The *Arabidopsis thaliana MERISTEM LAYER 1* promoter specifies epidermal expression in meristems and young primordia. *Plant J.* **20,** 259–263 (1999).
19. Wisman, E., Cardon, G. H., Fransz, P. & Saedler, H. The behaviour of the autonomous maize transposable element *En/Spm* in *Arabidopsis thaliana* allows efficient mutagenesis. *Plant Mol. Biol.* **37,** 989–999 (1998).
20. Kempin, S. A. *et al.* Targeted disruption in *Arabidopsis*. *Nature* **389,** 802–803 (1997).
21. Kunst, L., Klenz, J. E., Martinezzapater, J. & Haughn, G. W. *AP2* gene determines the identity of perianth organs in flowers of *Arabidopsis thaliana*. *Plant Cell* **1,** 1195–1208 (1989).
22. Yanofsky, M. F. *et al.* The protein encoded by the *Arabidopsis* homeotic gene *AGAMOUS* resembles transcription factors. *Nature* **346,** 35–39 (1990).

Supplementary Information accompanies the paper on **www.nature.com/nature**.

Acknowledgements We thank A. Ray for advice on scanning electron microscopy, D. Weigel for providing the pDW137 vector, members of Yanofsky laboratory for comments, and H. Chang and P. Golshani for technical assistance. A.P. received a scholarship from the Ananda Mahidol Foundation, and this work was supported by a grant from the National Science Foundation (to M.Y.).

Competing interests statement The authors declare that they have no competing financial interests.

Correspondence and requests for materials should be addressed to M.Y. (marty@ucsd.edu).

Selective imprinting of gut-homing T cells by Peyer's patch dendritic cells

J. Rodrigo Mora*, Maria Rosa Bono†, N. Manjunath*, Wolfgang Weninger*, Lois L. Cavanagh*, Mario Rosemblatt† & Ulrich H. von Andrian*

** The Center for Blood Research and Department of Pathology, Harvard Medical School, Boston, Massachusetts 02115, USA*
† Laboratorio de Inmunología, Facultad de Ciencias, Universidad de Chile, Fundación Ciencia para la Vida, and Millennium Institute for Fundamental and Applied Biology (MIFAB), Santiago 6842301, Chile

Whereas naive T cells migrate only to secondary lymphoid organs[1,2], activation by antigen confers to T cells the ability to home to non-lymphoid sites[3,4]. Activated effector/memory T cells migrate preferentially to tissues that are connected to the secondary lymphoid organs where antigen was first encountered[5–7]. Thus, oral antigens induce effector/memory cells that express essential receptors for intestinal homing, namely the integrin α4β7 and CCR9, the receptor for the gut-associated chemokine TECK/CCL25 (refs 6, 8, 9). Here we show that this imprinting of gut tropism is mediated by dendritic cells from Peyer's patches. Stimulation of CD8-expressing T cells by dendritic cells from Peyer's patches, peripheral lymph nodes and spleen induced equivalent activation markers and effector activity in T cells, but only Peyer's patch dendritic cells induced high levels of α4β7, responsiveness to TECK and the ability to home to the small

intestine. These findings establish that Peyer's patch dendritic cells imprint gut-homing specificity on T cells, and thus license effector/memory cells to access anatomical sites most likely to contain their cognate antigen.

It has been suggested that, during antigen stimulation of naive lymphocytes, the lymphoid tissue microenvironment provides instructions for peripheral homing preference[1,5,6]. However, this concept has been questioned[10]. We reasoned that, if antigen presentation has a lymphoid-organ-specific 'flavour', tissue tropism might be conferred to naive T cells by professional antigen-presenting cells, particularly dendritic cells (DCs). Thus, we analysed CD8-expressing ($CD8^+$) T cells from P14 × T-GFP mice that were stimulated *in vitro* by antigen-pulsed DCs from different lymphoid tissues. The P14 transgenic T-cell receptor (TCR) recognizes the $gp_{33–41}$ peptide from lymphocytic choriomeningitis virus (LCMV) in H-$2D^b$ (major histocompatibility complex (MHC) class I). In P14 × T-GFP mice, TCR-transgenic naive T cells express green fluorescent protein (GFP), whereas differentiated cytotoxic T lymphocytes (CTLs) downregulate GFP, providing a marker to distinguish effector cells from non-effector subsets[4].

To expand DCs in lymphoid tissues, donor mice were implanted subcutaneously with melanoma cells that secrete Flt3-L (FMS-like tyrosine kinase 3 ligand)[11]. Two weeks later, DCs were isolated from lymphoid organs by immunomagnetic depletion of other haematopoietic lineages. DCs were pulsed with $gp_{33–41}$ peptide and co-cultured with naive $CD8^+$ P14 × T-GFP cells. One week later, $CD8^+$ cells that had been stimulated by DCs from Peyer's patches (PP), peripheral lymph nodes (PLN) and spleen (henceforth referred to as $CD8^{PP\text{-}DC}$, $CD8^{PLN\text{-}DC}$ and $CD8^{Sp\text{-}DC}$, respectively) had more than doubled in number, expressed low levels of GFP (GFP^{low}) or were GFP-negative (GFP^-), expressed several common activation markers and displayed the 1B11 epitope of CD43, which distinguishes effector CTLs from naive and resting memory $CD8^+$ cells (Table 1 and Fig. 1). Indeed, $CD8^{PP\text{-}DC}$, $CD8^{PLN\text{-}DC}$ and, to a slightly lesser degree, $CD8^{Sp\text{-}DC}$ exerted antigen-specific cytotoxicity and produced interleukin-2 (IL-2) and interferon-γ on restimulation. Thus, all three DC populations generated bona fide effector CTLs.

Despite these functional and phenotypic similarities, there was a striking difference in α4β7 integrin expression. Although all stimulated T-cell populations expressed higher levels of α4β7 than did naive T cells, cells that expressed high levels of α4β7 ($\alpha4\beta7^{high}$ cells) were much more frequent among $CD8^{PP\text{-}DC}$ cells than among $CD8^{PLN\text{-}DC}$ or $CD8^{Sp\text{-}DC}$. This difference was apparent whether DCs were enriched by negative selection (85–90% $CD11c^+$) or purified by FACS sorting (>98% $CD11c^+$; Supplementary Fig. S-1a, b). By contrast, $\alpha4\beta7^{high}$ T cells were not increased when the sorted $CD11c^-$ fraction from enriched PP DCs was added to $CD8^+$ cells during stimulation with anti-CD3/CD28 (Supplementary Fig. S-1c) or with PLN DCs or spleen DCs (not shown). Thus, the induction of $\alpha4\beta7^{high}$ CTLs was mediated by DCs and not by other components of PP.

This unique effect of PP DCs is significant because only $\alpha4\beta7^{high}$ effector cells can attach efficiently to MAdCAM-1 (mucosal vascular addressin cell-adhesion molecule 1), which is constitutively expressed at relatively low density in intestinal microvessels[12,13]. Indeed, α4β7 levels comparable to those on $CD8^{PP\text{-}DC}$ cells were found on subsets of $TCR\alpha\beta^+CD8\alpha\beta^+$ memory cells in murine spleen and small intestine (not shown). However, it is unlikely that peptide-pulsed PP DCs expanded selectively the rare $\alpha4\beta7^{high}$ memory cells within the P14 × T-GFP starting population, because induction of α4β7 was equivalent when PP DCs were co-cultured with $\alpha4\beta7^-$ naive $CD8^+$ P14 × T-GFP cells that were sorted to >99% purity (Supplementary Fig. S-2). Moreover, 90% of $\alpha4\beta7^{high}$ $CD8^{PP\text{-}DC}$ cells expressed the P14 TCR, as assessed by staining with $gp_{33–41}$H-$2D^b$ MHC class I tetramer (Supplementary Fig. S-3). Also, PP DCs induced high levels of α4β7 on ovalbumin-specific T cells from OT-I × $Rag^{-/-}$ mice (Supplementary Fig. S-5a), in which conventional effector/memory cells are absent[14]. Thus, PP DCs did not merely expand memory cells that may have been preprogrammed for homing to the gut, but induced intestinal homing receptors during a primary T-cell response independent of TCR specificity.

Week-long exposure of T cells to DCs from any lymphoid tissue induced higher α4β7 levels than were observed on naive T cells. This is consistent with a recent report that T-cell activation with anti-CD3 enhanced α4β7 levels, and expression increased further in the presence of mesenteric lymph node (MLN) DCs[15]. On the other hand, whereas $\alpha4\beta7^{high}$ CTLs arose *in vitro* only after >4 days (not shown), immunization *in vivo* upregulates α4β7 on $CD4^+$ cells within 2 days, and only in intestinal lymphoid tissues, whereas $CD4^+$ cells in cutaneous lymph node downregulate α4β7 (ref. 7). This suggests that, in intact lymphoid organs, additional factors that are not fully recapitulated in our system might modulate the kinetics and tissue specificity of α4β7 induction.

Nevertheless, the difference in α4β7 staining between $CD8^{PP\text{-}DC}$ and other CTL populations was highly specific, as it was most apparent with the monoclonal antibody (MAb) DATK32, which recognizes the α4β7 heterodimer[16] (Table 1). Differences in the individual α4 and β7 chains were less pronounced, presumably because these subunits can also dimerize with integrins β1 and αE, respectively[17]. Indeed, β1 integrins were only modestly higher on $CD8^{PP\text{-}DC}$, whereas αE expression was similar on all CTL

Table 1 **Surface phenotype of naive and activated P14 × T-GFP cells**

	$CD8^{PP\text{-}DC}$	$CD8^{PLN\text{-}DC}$	$CD8^{Sp\text{-}DC}$	$CD8^{naive}$
Cell number ($\times10^6\,ml^{-1}$)	2.2 ± 0.6	2.7 ± 0.8	2.7 ± 0.9	NA
$Gp_{33–41}$H-$2D^b$ tetramer binding (%)	88 ± 3	92 ± 1	87 ± 5	80 ± 13
TCR-Vα2 chain (%)	168 ± 49 (93 ± 2)	177 ± 45 (94 ± 1)	128 ± 10 (94 ± 1)	190 ± 8 (92 ± 5)
CD25	174 ± 76	180 ± 81	122 ± 90	3 ± 2***
CD44	996 ± 367	891 ± 342	962 ± 211	115 ± 16***
CD122	18 ± 4	19 ± 6	14 ± 3	4 ± 1***
CD69 (%)	25 ± 10 (17 ± 8)	34 ± 15 (23 ± 14)	35 ± 13 (32 ± 14)	5 ± 1*** (3 ± 1)***
1B11/CD43	363 ± 192	393 ± 249	447 ± 279	70 ± 26***
L-selectin (%)	51 ± 33 (26 ± 9)	78 ± 51 (30 ± 10)	128 ± 98** (39 ± 8)**	319 ± 103*** (95 ± 4)***
GFP	31 ± 9	41 ± 17	54 ± 26	316 ± 82***
LFA-1	861 ± 321	970 ± 381	1,024 ± 396	319 ± 98***
β1 integrin	177 ± 17	142 ± 16*	134 ± 13*	14 ± 10***
αE integrin (%)	284 ± 108 (82 ± 11)	282 ± 113 (74 ± 13)	238 ± 61 (70 ± 13)	72 ± 68*** (43 ± 28)***
α4β7 heterodimer (% $\alpha4\beta7^{high}$)	165 ± 68 (52 ± 12)	65 ± 21*** (16 ± 8)***	49 ± 25*** (9 ± 6)***	15 ± 8*** (0.3 ± 0.2)***
α4 integrin	137 ± 93	71 ± 41**	69 ± 43**	31 ± 18***
β7 integrin	598 ± 184	468 ± 141	382 ± 106*	139 ± 90***
PSGL-1	69 ± 17	55 ± 18	60 ± 18	18 ± 5***

Results for $gp_{33–41}$H-$2D^b$ tetramer staining are shown as percentage of binding cells. Mean fluorescence intensity (MFI) of markers for T-cell activation (CD25, CD44, CD122, CD45RB, CD69), effector differentiation (GFP, 1B11) and adhesion molecules were measured on freshly isolated naive T cells and DC-stimulated effector cells (day 6–7) after gating on $CD8\alpha^+$ T cells in 10–22 independent experiments (mean ± s.d.). When two distinct populations were present, the percentage of positive cells is shown in parentheses. *$P < 0.05$, **$P < 0.01$, ***$P < 0.001$ compared with $CD8^{PP\text{-}DC}$. NA, not applicable; PSGL-1, P-selectin glycoprotein ligand-1.

populations. Likewise, the β2 integrin LFA-1 (lymphocyte-function-associated antigen) was upregulated equally in all CTL samples, whereas L-selectin, a homing receptor for PLN, was uniformly downregulated.

Next, we asked whether other gut-specific traffic molecules are preferentially modulated by PP DCs. In particular, CCR9, the receptor for TECK, has been implicated in T-cell migration to the small intestine[9,18,19]. Because antibodies to murine CCR9 were unavailable, we compared CTL migration towards a TECK gradient (Fig. 2a). $CD8^{PLN\text{-}DC}$ and $CD8^{Sp\text{-}DC}$ migrated poorly to TECK, whereas $CD8^{PP\text{-}DC}$ responded well to this chemokine. This effect was consistently induced by immunomagnetically enriched and FACS-purified PP DCs (Supplementary Fig. S-4), and was also observed with OT-I × $RAG^{-/-}$ T cells (Supplementary Fig. S-5b). By contrast, all CTL populations responded equally to several other lymphoid and inflammatory chemokines (Fig. 2b).

As shown previously, naive $CD8^{+}$ cells also migrated towards TECK[20]. Their response was even greater than that of $CD8^{PP\text{-}DC}$. This suggests that DCs from PLN and spleen induced a loss of CTL responsiveness to TECK that was partially prevented or reversed by PP DCs. Accordingly, naive T cells expressed more CCR9 messenger RNA than did CTLs (Fig. 2c). Interestingly, CCR9 mRNA levels were lower in $CD8^{PLN\text{-}DC}$ than in $CD8^{PP\text{-}DC}$, but they were equivalent in $CD8^{PP\text{-}DC}$ and $CD8^{Sp\text{-}DC}$. Thus, differential transcriptional regulation of CCR9 explains only partially the observed differences in chemotactic efficacy of TECK. This implies a role for post-transcriptional regulation of CCR9 expression or function, analogous to that reported previously for CCR6 (ref. 21).

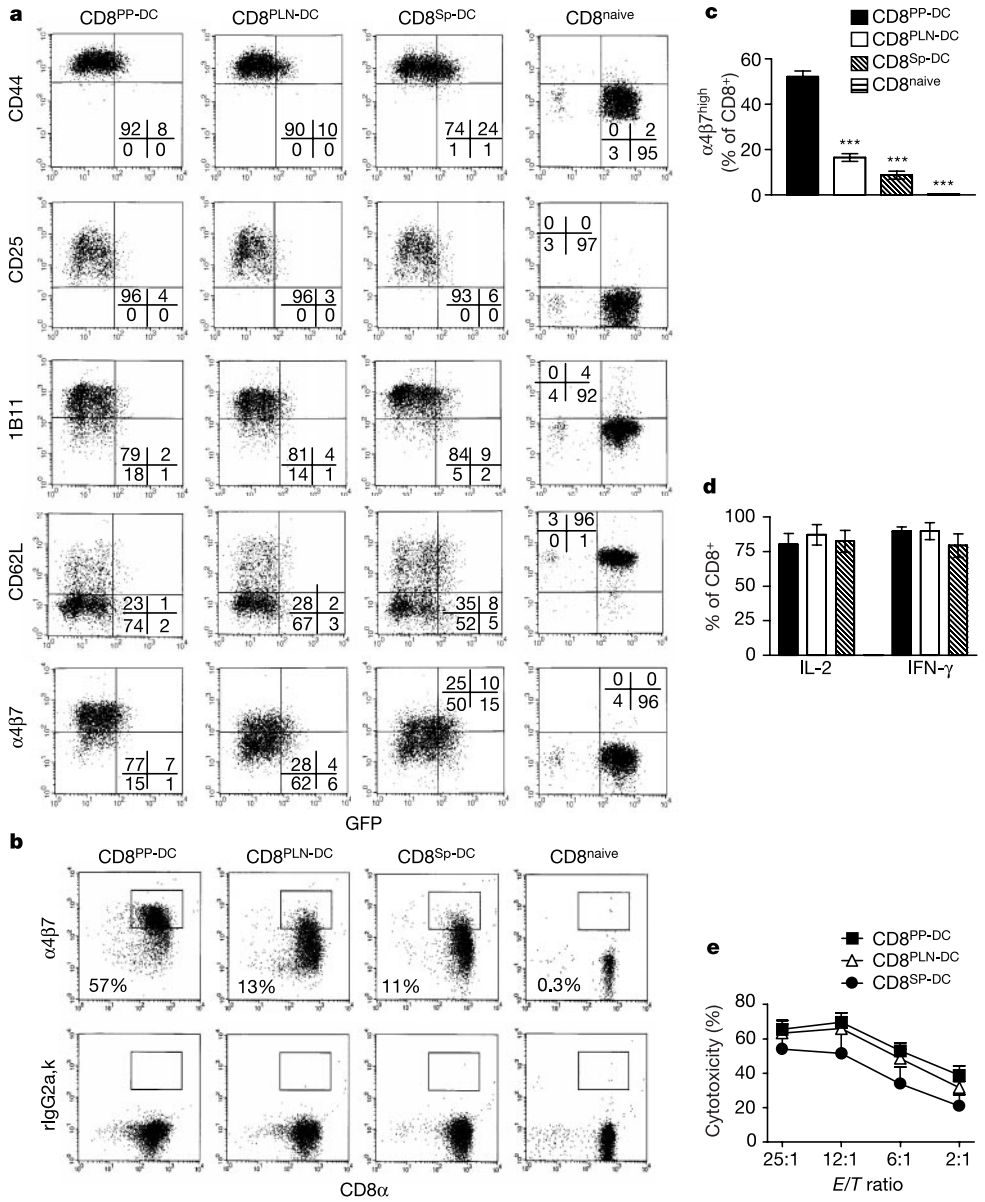

Figure 1 Antigen stimulation of $CD8^{+}$ cells by DCs from PP, spleen and PLN induces equivalent activation markers and effector activity, but only PP DCs induce high expression of α4β7 integrin. P14 × T-GFP cells were cultured for 6–7 days with $gp_{33–41}$-pulsed DCs from different lymphoid organs, and their surface phenotype was compared with naive $CD8^{+}$ P14 × T-GFP cells by flow cytometry. **a**, Representative histograms for CD25, CD44, 1B11, L-selectin (CD62L) and α4β7 compared with GFP. **b**, Representative staining of α4β7 heterodimer (top row) and isotype-matched control MAb (bottom row) versus CD8α. Numbers in histograms reflect the frequency of cells in the $CD8^{+}\alpha4\beta7^{high}$ gate (rectangles). **c**, Statistical analysis shows that the frequency of $CD8^{+}\alpha4\beta7^{high}$ cells was significantly higher in cells stimulated by PP DCs ($n = 22$ for $CD8^{PP\text{-}DC}$ and $CD8^{PLN\text{-}DC}$, 8 for $CD8^{Sp\text{-}DC}$ and 9 for naive; $^{***}P < 0.001$ compared with $CD8^{PP\text{-}DC}$). By contrast, all DC populations induced equivalent effector functions as evidenced by **d**, the production of cytokines induced by phorbol 12-myristate 13-acetate/ionomycin ($n = 3$) and **e**, antigen-specific cytotoxicity ($n = 3$). E/T ratio, effector-to-target ratio.

Table 2 **Phenotype of DCs from PP, PLN and spleen**

	PP DCs		PLN DCs		Spleen DCs	
	$CD8\alpha^+$	$CD8\alpha^-$	$CD8\alpha^+$	$CD8\alpha^-$	$CD8\alpha^+$	$CD8\alpha^-$
% of DC subset	38 ± 14	62 ± 14	61 ± 14**	39 ± 14**	48 ± 8	52 ± 8
H-$2K^b$ (MHC class I)	148 ± 72	122 ± 61	183 ± 42	165 ± 50	142 ± 22	109 ±21
I-A/I-E (MHC class II)	770 ± 326	808 ± 303	844 ± 155	1,256 ± 310	740 ± 266	569 ± 236
CD40	5 ± 2	3 ± 2	3 ± 5	3 ± 5	4 ± 2	1 ± 3
CD80	41 ± 17	25 ± 6	22 ± 5*	21 ± 7	24 ± 5	15 ± 4*
CD86	13 ± 9	10 ± 5	12 ± 5	12 ± 5	11 ± 4	6 ± 2
CD1d (%)	30 ± 5 (58 ± 10)	25 ± 1 (46 ± 9)	41 ± 11 (77 ± 1)	31 ± 1 (50 ± 4)	81 ± 32 (91 ± 3)	33 ± 8 (56 ± 1)
CD48	840 ± 28	701 ± 14	1,025 ± 12	955 ± 42	784 ± 109	656 ± 60
ICAM-1	504 ± 9	390 ± 23	500 ± 35	416 ± 52	515 ± 119	260 ± 39

Data are mean ± s.d. of MFI (or percentage of marker-positive cells) after gating on $CD11c^+CD8\alpha^+$ or $CD11c^+CD8\alpha^-$ cells. $n \geq 3$ independent DC preparations. *$P < 0.05$, **$P < 0.01$ compared with corresponding PP DC subset. ICAM-1, intercellular adhesion molecule 1.

As α4β7 and CCR9 are essential intestinal homing receptors[9,18,22], we postulated that adoptively transferred $CD8^{PP\text{-}DC}$ should home to the gut. To test this, we performed competitive homing experiments by injecting into non-transgenic recipients a mixture of naive T-GFP cells and $CD8^{PP\text{-}DC}$ or $CD8^{PLN\text{-}DC}$ stained with tetramethylrhodamine isothiocyanate (TRITC), a red fluorophor. The homing index in recipient tissues (the ratio of $TRITC^+$ to GFP^+ cells, corrected for input) was determined 4 h later (Fig. 3a). Compared with naive T cells, $CD8^{PP\text{-}DC}$ and $CD8^{PLN\text{-}DC}$ homed poorly to lymph nodes, whereas all three T-cell populations had equivalent spleen-homing abilities. The two CTL populations accumulated in the liver and lungs in much larger numbers than naive T cells. This migratory behaviour is typical for naive and effector $CD8^+$ cells[23]. Interestingly, although $CD8^{PP\text{-}DC}$ migrated less than naive T cells to PP (about threefold when corrected for circulating cell counts), $CD8^{PP\text{-}DC}$ homed to PP significantly better than $CD8^{PLN\text{-}DC}$. Conversely, $CD8^{PLN\text{-}DC}$ retained a higher capacity than $CD8^{PP\text{-}DC}$ to home to skin-draining PLN.

We also counted homed T cells in the lamina propria (LP) and among intra-epithelial lymphocytes (IEL) in the small intestine. In most cases, GFP^+ naive T cells were undetectable in these tissues, whereas $CD8^{PP\text{-}DC}$ cells were routinely recovered. Because the absence of naive T cells prohibited us from calculating intestinal homing indices, we carried out further competitive homing experiments with differentially labelled $CD8^{PLN\text{-}DC}$ and $CD8^{PP\text{-}DC}$ (Fig. 3b). The ratio of $CD8^{PP\text{-}DC}$ to $CD8^{PLN\text{-}DC}$ was 17 ± 6 times (mean ± s.e.m.) higher in the small intestine than in the blood. Comparably pronounced differences were also observed when the fluorescent dyes were switched (not shown), or when $CD8^{PP\text{-}DC}$ and $CD8^{PLN\text{-}DC}$ were generated from OT-I × $RAG^{-/-}$ mice (Supplementary Fig. S-5c). There was a significant positive correlation between the ratio of α4β7 staining on $CD8^{PP\text{-}DC}$ versus $CD8^{PLN\text{-}DC}$, and the homing index in the small intestine (Fig. 3c), indicating that the induction of $\alpha4\beta7^{high}$ T cells by PP DCs is a prerequisite mechanism for effector-cell targeting to that organ. Furthermore, in two independent experiments, a neutralizing MAb to TECK reduced the homing index by 51% compared with an isotype-matched control MAb. Thus, consistent with a recent report[9], responsiveness to TECK is required for efficient effector-cell homing to the small intestine (Supplementary Fig. S-6).

$CD8^{PP\text{-}DC}$ homed significantly more to PP and MLN than did $CD8^{PLN\text{-}DC}$ (Fig. 3b), but these differences were comparatively modest. On the other hand, the superior homing ability of $CD8^{PP\text{-}DC}$ over $CD8^{PLN\text{-}DC}$ was specific for the digestive tract, as their concentration was similar in blood, lung and spleen. Interestingly, despite their pronounced tropism for the small intestine, $CD8^{PP\text{-}DC}$ migrated poorly to the colon, similar to $CD8^{PLN\text{-}DC}$ (homing index, 1.3 ± 0.2). This observation lends experimental support to the notion that the small and large bowel have distinct homing requirements[24].

Previous work has shown that individual DC subsets can bias T-cell differentiation, and DCs from different lymphoid organs can elicit distinct T-cell responses[25,26]. For example, PLN DCs and PP DCs polarize $CD4^+$ cells preferentially towards a T_H1 and T_H2 (T helper cell) phenotype, respectively[25,26]. Thus, it was important to assess whether PP DCs exerted a similar effect on $CD8^+$ cells, as *in vitro* polarized T_C1 and T_C2 (T cytotoxic) cells have distinct migratory properties[27]. However, $CD8^{PP\text{-}DC}$ and $CD8^{PLN\text{-}DC}$ underwent comparable effector differentiation (Fig. 1d, e). Thus, the selective ability of PP DCs to confer gut tropism was not mirrored in a distinct capacity to induce polarized CTL responses.

We also examined the composition of DCs, as normal lymphoid

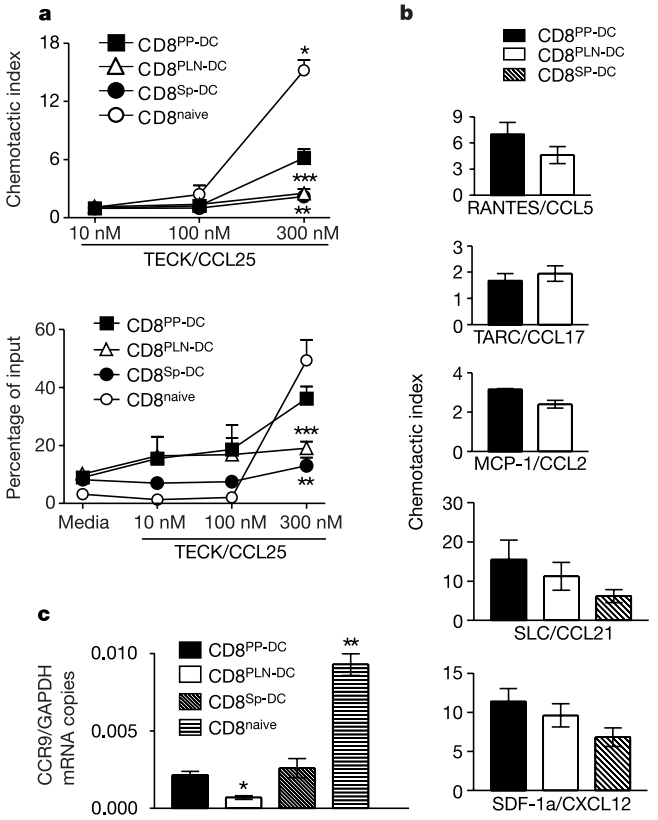

Figure 2 $CD8^{PP\text{-}DC}$ are significantly more responsive than $CD8^{PLN\text{-}DC}$ or $CD8^{Sp\text{-}DC}$ to the gut-associated chemokine TECK/CCL25. **a**, P14 × T-GFP cells were cultured for 6–7 days with gp_{33-41}-pulsed DCs isolated from different lymphoid tissues and compared with naive P14 × T-GFP cells in Transwell chemotaxis assays using different concentrations of TECK (n = 6–22). Data are shown as chemotactic index; that is, the number of cells migrated towards TECK normalized to the number migrated towards medium (top), and as percentage of input cells recovered from the bottom chamber (bottom). **b**, Migration towards an optimum concentration of RANTES/CCL5, SDF/CXCL12, SLC/CCL21, MCP-1/CCL2 and TARC/CCL17. **c**, Real-time RT–PCR of CCR9 mRNA relative to GAPDH mRNA in $CD8^+$ effector cells and purified naive P14 × T-GFP T cells (n = 2–3). *$P < 0.05$, **$P < 0.01$, ***$P < 0.001$ compared with $CD8^{PP\text{-}DC}$.

tissues contain several DC subsets with distinct expression patterns of CD8α and CD11b[25]. In Flt3-L-treated donors, PP contained fewer CD8α$^+$ DCs than did PLN (Table 2). However, CD8α$^+$ DCs were equally represented in PP and spleen, and depletion of CD8α$^+$ cells from PP DCs and PLN DCs did not alter their differential effect on α4β7 expression and TECK responsiveness by T cells (not shown). All DC populations showed similar levels of co-stimulatory and classical MHC molecules as well as non-classical MHC molecules such as Qa-1 and Qa-2, which have been implicated in intestinal targeting of CD8$^+$ recent thymic emigrants[28] (not shown). Thus, the mechanism(s) by which PP DCs confer tissue specificity remain(s) to be identified.

After a T cell has been activated in PP, it returns by way of efferent lymph, MLN and the thoracic duct to the blood stream, and then homes to the gut mucosa to establish a first line of defence against recurrent intestinal pathogens[5]. Of note, CD8$^{PP\text{-}DC}$ accumulated in non-inflamed gut. Thus, they followed constitutively expressed traffic signals provided, at least in part, by MAdCAM-1/α4β7 and TECK/CCR9. Inflammatory mediators induce a plethora of further recruitment pathways[1,2,4]. Our analysis shows that DCs from any lymphoid organ prompt CTLs to upregulate an arsenal of traffic molecules to respond to such inflammatory signals. Thus, intestinal inflammation would probably not only amplify CTL recruitment, but may also lessen the requirement for migratory specialization.

Although antigen-induced default changes in common inflammatory traffic molecules on T cells are well established[1,2,4], our findings reveal a novel, tissue-specific aspect of DC-induced effector/memory cell differentiation. We show that PP DCs can target activated CD8$^+$ cells to the small intestine, whereas other DCs do not have this ability. We have also observed that PP DCs upregulate α4β7 expression on CD4$^+$ cells (J.R.M., M.R.B. and M.R., unpublished observation). As their intestine-specific character was maintained after PP DCs were transferred into tissue culture, it seems unlikely that additional microenvironmental signals (such as stroma cells) are crucial for tissue-specific imprinting, at least in PP. However, local environmental cues probably provide necessary differentiation signals to DCs or DC precursors that enter PP. Whether DCs in other lymphoid organs have effector-targeting properties for associated peripheral tissues remains to be tested.

It will also be interesting to determine whether PP DCs confer gut tropism by selection or instruction. In a scenario governed by selection, T cells initiate random differentiation programmes that result in diverse tissue specificity, and appropriate subsets are then selected by DCs to proliferate and/or survive[10]. Alternatively, PP DCs may provide differentiation signals a priori to induce α4β7 and possibly CCR9. In our experiments, DCs rapidly disappeared from co-cultures and were essentially absent after day 3, whereas α4β7^{high} CD8$^{PP\text{-}DC}$ arose only after day 4. This observation is more easily reconciled with an instructive mechanism and supports the view that tissue-specific T-cell memory reflects differentiation concurrent with the activation process rather than post-activation selection. □

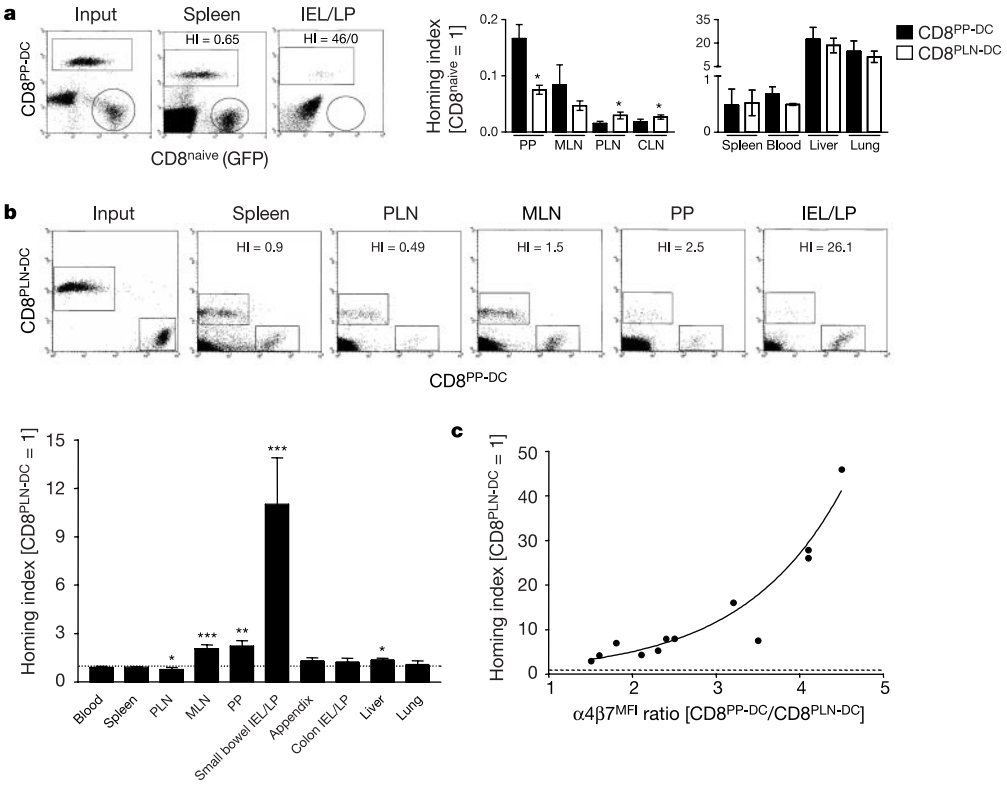

Figure 3 CD8$^{PP\text{-}DC}$ home to the small intestine. P14 × T-GFP cells were cultured for 6–7 days with gp$_{33–41}$-pulsed DCs isolated from PLN or PP of the same donor pool. **a**, In one series, stimulated cells were labelled with TRITC and mixed with an equal number of T-GFP cells (containing ~35% GFP$^+$ naive T cells), and the homing index (HI, the ratio of [TRITC$^+$ cells] to [GFP$^+$ cells] in recipient blood or tissues divided by the input ratio) was determined in recipients' blood and tissues 4 h after adoptive transfer. FACS histograms (left) show a representative experiment comparing CD8$^{PP\text{-}DC}$ and naive T-GFP cells (non-fluorescent input cells are non-T cells among donor splenocytes). Bar graphs (right) show mean ± s.e.m. of three experiments (*, $P < 0.05$ compared with CD8$^{PP\text{-}DC}$). **b**, In a second series, CD8$^{PP\text{-}DC}$ and CD8$^{PLN\text{-}DC}$ were mixed after staining with calcein AM (or CFSE) and TRITC, respectively, and the HI (the ratio of [calcein$^+$ (or CFSE$^+$)] to [TRITC$^+$], corrected for input) was determined 24 h later. Histograms from a representative experiment and mean ± s.e.m. of all experiments are shown ($n = 3–12$; *$P < 0.05$, **$P < 0.01$, ***$P < 0.001$ compared with HI = 1). **c**, Correlation between the ratios of α4β7 expression on CD8$^{PP\text{-}DC}$ compared with CD8$^{PLN\text{-}DC}$ and the HI of both populations in small intestine ($r^2 = 0.95$, $P < 0.0001$). The broken line represents HI = 1.

Methods

For a detailed description of methods used in this study, see Supplementary Information.

Mice and reagents

C57BL/6 mice were obtained from Jackson Labs. T-GFP and P14 × T-GFP mice have been described previously[4]. OT-I × RAG$^{-/-}$ mice, ovalbumin-derived SIINFEKEL peptide and Flt3-L transfectants were provided by H. Ploegh. Mice were housed in a SPF/VAF (specific-pathogen-free and viral-antibody-free) facility and used between 8–16 weeks of age in accordance with National Institutes of Health guidelines. MAbs and cytokine staining kits were from Pharmingen. LCMV $gp_{33–41}$ peptide (KAVYNFATC) was from Biosource. Murine rIL-2 and chemokines were from R&D Systems.

DC isolation

Female C57BL/6 mice were injected subcutaneously with B16 melanoma cells secreting Flt3-L[11]. After 12–17 days, mice were killed and single-cell suspensions were generated by digesting PP, PLN and spleen with collagenase D and DNase I (Roche). DCs were immunomagnetically isolated by negative selection using MAbs to B220, CD3, CD19, Pan-NK, Ter-119, Ly-6G and Thy-1[29], and goat anti-rat IgG microbeads (Miltenyi Biotec). Negatively selected DCs were pulsed with 10 μg ml^{-1} $gp_{33–41}$ or SIINFEKL peptide in IMDM with standard supplements and 10% FBS (complete IMDM), and used immediately in co-cultures. For some experiments, negatively selected DCs were stained with fluorescein isothiocyanate (FITC)–anti-CD11c and a cocktail of phycoerythrin (PE)-labelled lineage-specific antibodies, and sorted into CD11c$^+$ and CD11c$^-$ fractions using a FACS Vantage cell sorter (Becton Dickinson). Sorted cells were pulsed with peptide and used as described above.

T-cell isolation and T-cell/DC co-cultures

Naive CD8$^+$ P14 × T-GFP and OT-I × Rag$^{-/-}$ T cells were purified from splenocytes by red blood cell lysis ('ACK' lysis buffer) followed by negative immunomagnetic selection using MAbs to B220, I-A/I-E, CD4, CD19, Pan-NK, Ter-119 and Ly-6G, as described above. T cells (90–95% CD8$^+$, L-selectin^{high}, CD44^{low}, GFP^{high}) were co-cultured with 1×10^6 peptide-pulsed DCs (ratio of T cells to DCs, 1:1 or 2:1) from different lymphoid organs in 3 ml of complete IMDM using 12-well tissue-culture treated plates (Falcon). On day 3, 2 ml of complete IMDM and a single dose of 10 ng ml^{-1} IL-2 were added to maintain viability, and 2 ml of complete IMDM were replaced daily thereafter. Cells were used after 6–7 days in culture. For some experiments, naive P14 × T-GFP cells were stimulated with and without the addition of sorted CD11c$^+$ or CD11c$^-$ fractions. For this, 12-well plates were coated with anti-CD3 and anti-CD28, and CD8$^+$ P14 × T-GFP cells were added alone or together with sorted CD11c$^+$ or CD11c$^-$ cells (ratio of T cells to sorted cells, 1:1 or 2:1). After 3 days in culture, T cells were transferred to plates without antibodies and maintained as described above.

Characterization of CTL phenotype

The surface phenotype and intracellular cytokine production of differentiated T-cell populations were analysed on a FACScan flow cytometer (Becton Dickinson) using standard techniques. To assess antigen-specific cytotoxicity, a 6 h chromium release assay was carried out as described[30]. To measure CCR9 mRNA levels, the ratio of message levels for CCR9 and the housekeeping gene GAPDH (glyceraldehyde-3-phosphate dehydrogenase) was determined by real-time RT–PCR (polymerase chain reaction with reverse transcription) using an iCycler(Bio-Rad) and the SYBR Green DNA PCR Core Kit (Applied Biosystems).

Chemotaxis assay

A standard 90 min chemotaxis assay with Transwell filters (pore size, 5 μm) was used to assess CTL responsiveness to different chemokines[23]. Chemotactic indices were calculated as the number of migrated cells in wells containing chemokine, divided by the number of migrated cells in wells containing medium alone. The percentage of migrated cells relative to cells in the input was also determined.

Homing assay

Competitive homing experiments of TRITC-labelled CD8^{PLN-DC} and CD8^{PP-DC} cells and naive T-GFP splenocytes were performed as described elsewhere[23]. Briefly, 2×10^7 CTLs were mixed with the same number of T-GFP cells and injected intravenously into non-transgenic recipients. An aliquot was saved to assess the input ratio ($IR = [TRITC^+]_{input}/[GFP^+]_{input}$). After 4 h, recipient tissues were harvested to measure TRITC$^+$/GFP$^+$ ratios by flow cytometry. The homing index, HI, was calculated as the ratio of $[TRITC^+]_{tissue}/[GFP^+]_{tissue}$ to IR. To compare the migration of CD8^{PLN-DC} and CD8^{PP-DC}, one population was labelled with TRITC (Molecular Probes) and the other with calcein AM or CFSE (Molecular Probes). 2×10^7 cells from each population were mixed and used for competitive homing experiments. In two experiments, mice were injected with 100 μg rIgG2b or anti-TECK/CCL25 (R&D Systems, clone 89818) 4 h before and during CTL injection. Recipients were sacrificed after 18 h and lymphocytes from LP and IEL were obtained as described[3]. The HI was calculated as the ratio of $[CD8^{PP-DC}]_{tissue}/[CD8^{PLN-DC}]_{tissue}$ to $[CD8^{PP-DC}]_{input}/[CD8^{PLN-DC}]_{input}$.

Statistical analysis

Data are presented as mean ± s.e.m. and were analysed using either the Kruskal-Wallis test with Dunn's post-test or one-way ANOVA with Bonferroni correction, as appropriate. Homing indices were tested versus HI = 1 using a one-sample Wilcoxon-signed rank test. Significance was set at $P < 0.05$.

Received 14 January; accepted 12 March 2003; doi:10.1038/nature01726.

1. Butcher, E. C., Williams, M., Youngman, K., Rott, L. & Briskin, M. Lymphocyte trafficking and regional immunity. *Adv. Immunol.* **72,** 209–253 (1999).
2. von Andrian, U. H. & Mackay, C. R. T-cell function and migration. Two sides of the same coin. *N. Engl. J. Med.* **343,** 1020–1034 (2000).
3. Masopust, D., Vezys, V., Marzo, A. L. & Lefrancois, L. Preferential localization of effector memory cells in nonlymphoid tissue. *Science* **291,** 2413–2417 (2001).
4. Weninger, W., Manjunath, N. & von Andrian, U. H. Migration and differentiation of CD8$^+$ T cells. *Immunol. Rev.* **186,** 221–233 (2002).
5. Guy-Grand, D., Griscelli, C. & Vassalli, P. The mouse gut T lymphocyte, a novel type of T cell. Nature, origin, and traffic in mice in normal and graft-versus-host conditions. *J. Exp. Med.* **148,** 1661–1677 (1978).
6. Kantele, A., Zivny, J., Hakkinen, M., Elson, C. O. & Mestecky, J. Differential homing commitments of antigen-specific T cells after oral or parenteral immunization in humans. *J. Immunol.* **162,** 5173–5177 (1999).
7. Campbell, D. J. & Butcher, E. C. Rapid acquisition of tissue-specific homing phenotypes by CD4$^+$ T cells activated in cutaneous or mucosal lymphoid tissues. *J. Exp. Med.* **195,** 135–141 (2002).
8. Hamann, A., Andrew, D. P., Jablonski-Westrich, D., Holzmann, B. & Butcher, E. C. Role of α_4-integrins in lymphocyte homing to mucosal tissues *in vivo*. *J. Immunol.* **152,** 3282–3293 (1994).
9. Svensson, M. *et al.* CCL25 mediates the localization of recently activated CD8αβ$^+$ lymphocytes to the small-intestinal mucosa. *J. Clin. Invest.* **110,** 1113–1121 (2002).
10. Davenport, M. P., Grimm, M. C. & Lloyd, A. R. A homing selection hypothesis for T-cell trafficking. *Immunol. Today* **21,** 315–317 (2000).
11. Shi, G. P. *et al.* Cathepsin S required for normal MHC class II peptide loading and germinal center development. *Immunity* **10,** 197–206 (1999).
12. Nakache, M., Berg, E. L., Streeter, P. R. & Butcher, E. C. The mucosal vascular addressin is a tissue-specific endothelial cell adhesion molecule for circulating lymphocytes. *Nature* **337,** 179–181 (1989).
13. Berlin, C. *et al.* α4 integrins mediate lymphocyte attachment and rolling under physiologic flow. *Cell* **80,** 413–422 (1995).
14. Schott, E. & Ploegh, H. L. Mouse MHC class I tetramers that are unable to bind to CD8 reveal the need for CD8 engagement in order to activate naive CD8 T cells. *Eur. J. Immunol.* **32,** 3425–3434 (2002).
15. Stagg, A. J., Kamm, M. A. & Knight, S. C. Intestinal dendritic cells increase T cell expression of α4β7 integrin. *Eur. J. Immunol.* **32,** 1445–1454 (2002).
16. Andrew, D. P. *et al.* Distinct but overlapping epitopes are involved in $\alpha_4\beta_7$-mediated adhesion to vascular cell adhesion molecule-1, mucosal addressin-1, fibronectin, and lymphocyte aggregation. *J. Immunol.* **153,** 3847–3861 (1994).
17. Hynes, R. O. Integrins: bidirectional, allosteric signaling machines. *Cell* **110,** 673–687 (2002).
18. Zabel, B. A. *et al.* Human G protein-coupled receptor GPR-9-6/CC chemokine receptor 9 is selectively expressed on intestinal homing T lymphocytes, mucosal lymphocytes, and thymocytes and is required for thymus-expressed chemokine-mediated chemotaxis. *J. Exp. Med.* **190,** 1241–1256 (1999).
19. Zaballos, A., Gutierrez, J., Varona, R., Ardavin, C. & Marquez, G. Cutting edge: identification of the orphan chemokine receptor GPR-9-6 as CCR9, the receptor for the chemokine TECK. *J. Immunol.* **162,** 5671–5675 (1999).
20. Carramolino, L. *et al.* Expression of CCR9 β-chemokine receptor is modulated in thymocyte differentiation and is selectively maintained in CD8$^+$ T cells from secondary lymphoid organs. *Blood* **97,** 850–857 (2001).
21. Iwasaki, A. & Kelsall, B. L. Localization of distinct Peyer's patch dendritic cell subsets and their recruitment by chemokines macrophage inflammatory protein (MIP)-3α, MIP-3β, and secondary lymphoid organ chemokine. *J. Exp. Med.* **191,** 1381–1394 (2000).
22. Wagner, N. *et al.* Critical role for β7 integrins in formation of the gut-associated lymphoid tissue. *Nature* **382,** 366–370 (1996).
23. Weninger, W., Crowley, M. A., Manjunath, N. & von Andrian, U. H. Migratory properties of naive, effector, and memory CD8$^+$ T cells. *J. Exp. Med.* **194,** 953–966 (2001).
24. Kunkel, E. J. & Butcher, E. C. Chemokines and the tissue-specific migration of lymphocytes. *Immunity* **16,** 1–4 (2002).
25. Kelsall, B. L., Biron, C. A., Sharma, O. & Kaye, P. M. Dendritic cells at the host–pathogen interface. *Nature Immunol.* **3,** 699–702 (2002).
26. Banchereau, J. *et al.* Immunobiology of dendritic cells. *Annu. Rev. Immunol.* **18,** 767–811 (2000).
27. Xie, H., Lim, Y. C., Luscinskas, F. W. & Lichtman, A. H. Acquisition of selectin binding and peripheral homing properties by CD4$^+$ and CD8$^+$ T cells. *J. Exp. Med.* **189,** 1765–1776 (1999).
28. Maurice, M. M., Gould, D. S., Carroll, J., Vugmeyster, Y. & Ploegh, H. L. Positive selection of an MHC class-I restricted TCR in the absence of classical MHC class I molecules. *Proc. Natl Acad. Sci. USA* **98,** 7437–7442 (2001).
29. Suss, G. & Shortman, K. A subclass of dendritic cells kills CD4 T cells via Fas/Fas-ligand-induced apoptosis. *J. Exp. Med.* **183,** 1789–1796 (1996).
30. Manjunath, N. *et al.* A transgenic mouse model to analyse CD8$^+$ effector T cell differentiation *in vivo*. *Proc. Natl Acad. Sci. USA* **96,** 13932–13937 (1999).

Supplementary Information accompanies the paper on **www.nature.com/nature**.

Acknowledgements We are grateful to H. Ploegh for providing reagents and mice. We thank I. Dodge, B. Harnisch, G. Cheng, N. Barteneva, C. Halin, E. Schott and S. Feske for advice and technical assistance. J.R.M. is indebted to Ingrid Ramos for constant support. This work was supported by grants from NIH to U.H.v.A.; from Fondecyt to J.R.M., M.R.B. and M.R.; and from MIFAB (financed in part by Ministerio de Planificación y Cooperación, Chile) to M.R. W.W. is a fellow of the Max Kade Foundation. J.R.M. was supported in part by fellowships from Fundación Andes and the Pew Foundation.

Competing interests statement The authors declare that they have no competing financial interests.

Correspondence and requests for materials should be addressed to U.H.v.A. (uva@cbr.med.harvard.edu).